Molecular mechanism of abnormally large nonsoftening deformation in a tough hydrogel

Ya Nan Ye, Kunpeng Cui, Wei Hong, Xueyu Li, Chengtao Yu, Dominique Hourdet, Tasuku Nakajima, Takayuki Kurokawa, Jian Ping Gong

Molecular mechanism of abnormally large non-softening deformation in a tough hydrogel

Ya Nan Ye[1], Kunpeng Cui[2], Wei Hong[1,3], Xueyu Li[1], Chengtao Yu[4], Dominique Hourdet[1,5], Tasuku Nakajima[1,2,6], Takayuki Kurokawa[1,6] and Jian Ping Gong[1,2,6*]*

[1]Global Institution for Collaborative Research and Education (GI-CoRE), Hokkaido University, Sapporo 001-0021 Japan,

[2]Institute for Chemical Reaction Design and Discovery (WPI-ICReDD), Hokkaido University, Sapporo 001-0021 Japan,

[3]Department of Mechanics and Aerospace Engineering, Southern University of Science and Technology, Shenzhen, Guangdong, 518055 China,

[4]Graduate School of Life Science, Hokkaido University, Sapporo 001-0021 Japan,

[5]Soft Matter Science and Engineering, ESPCI Paris, University PSL, CNRS, Sorbonne University, 75005 Paris, France,

[6]Faculty of Advanced Life Science, Hokkaido University, Sapporo 001-0021 Japan.

* Kunpeng Cui

Email: kpcui@sci.hokudai.ac.jp

* Jian Ping Gong

Email:gong@sci.hokudai.ac.jp

Classification

Physical Sciences, Applied Physical Sciences

Keywords

tough hydrogel, non-softening, large quasi-linear deformation, hyperconnective network, molecular glue, affine deformation

Author Contributions

Y.Y., K.C., and J. P. G. designed the experiments and performed the data analysis. Y.Y., and K.C. performed experiment. All authors participated in discussion. Y.Y., K.C., and J.P.G. wrote the manuscript.

The authors declare no competing interest.

This PDF file includes:

Main Text
Figs 1 to 4

Abstract

Tough soft materials usually show strain softening and inelastic deformation. Here we study the molecular mechanism of abnormally large non-softening, quasi-linear but inelastic deformation in tough hydrogels made of hyperconnective physical network and linear polymers as molecular glues to the network. The interplay of hyperconnectivity of network and effective load

transfer by molecular glues prevents stress concentration, which is revealed by an affine deformation of the network to the bulk deformation up to sample failure. The suppression of local stress concentration and strain amplification plays a key role in avoiding necking or strain softening and endows the gels with a unique large non-softening, quasi-linear but inelastic deformation.

Significance Statement

Tough soft materials usually show strain softening. Avoiding strain softening, although important for practical application, had not been a focus of research. Recently, a series of tough hydrogels made from hyperconnective physical networks and linear polymers as molecular glue show extraordinarily large non-softening, quasi-linear but inelastic deformation. Here, we studied the molecular mechanism of this behavior and clarified that it is a direct consequence of the interplay between hyperconnectivity of the skeleton network and the stress transfer through molecular glues. We believe that this work gives important insight on the design and development of tough soft materials without strain softening.

Introduction

Linear mechanical deformation is usually found in hard and brittle materials, such as in common glass and ceramics.(1, 2) In contrast, tough

materials, regardless of hard and soft, usually show a strong non-linear and inelastic tensile deformation, featured by strain softening and mechanical hysteresis.(3–8) The stress of a tough material often becomes prominently sub-linear or even exhibits a plateau at large strain. The latter behavior is sometimes called yielding (3, 9) or yielding-like phenomenon (10, 11). In general, the strain softening or yielding is caused by the structure damage or structure change, while the specific mechanism depends on materials.(7, 12–16) For example, a tough metal shows strain-softening along with a residual strain, which is associated to the sliding of crystalline plane and grain boundary.(3, 9) A tough double network (DN) hydrogel(8), consisting of a hard/brittle first network and a soft/stretchable second network interpenetrated, exhibits a stress plateau at large strain with negligible residual strain. The yielding-like phenomenon of a DN material is associated to the rupture of the first network into discontinuous phases through covalent bond breakage that is strain rate-independent. Local strain amplification occurs significantly above the yielding strain, and the network deformation largely deviates from the bulk deformation, which is called non-affine deformation.(17–20) The negligible permanent residual strain of the DN material is due to the elasticity of the second network.(21)

Recently, we developed a class of unique tough and strong hydrogels that do not show obvious strain softening or necking, instead, they show large quasi-linear but inelastic tensile deformation up to sample failure.(22) This class of gels, referred as glue-B gels, consist of a hyperconnective physical network and linear polymers. The hyperconnective network (referred as B gel) is made from amphiphilic triblock copolymers that form micelles by their hydrophobic end-blocks, and the micelles act as hyper-functional crosslinkers to connect tens of hydrophilic mid-blocks network strands (Fig. 1a). The linear polymers form physical bonds with the mid-blocks of the physical network, acting as molecular glues. The structures of these gels are significantly different from conventional tough DN hydrogels, in which each crosslinker usually connects four network strands by bifunctional crosslinkers and there is no appreciable inter-polymer association. These glue-B gels show mechanical hysteresis, as like other tough hydrogels. The B gel has a fracture energy around 60 J/m^2, while the corresponding glue-B gel reaches a value around 3000 J/m^2.(22)

In this work, we aim to clarify the molecular mechanism of the abnormally large non-softening, but inelastic tensile deformation and the high toughness of the glue-B gels. We find that the interplay of the hyperconnectivity of the

physical network and the stress transfer through the molecular glues effectively suppresses local stress concentration and strain amplification, which can be identified by the affine deformation of the network. The suppression of local stress concentration and strain amplification plays a key role in avoiding prominent strain softening or yielding and endows the gel a large quasi-linear deformation in a wide observation window.

Results and discussion

The B gels were prepared from the amphiphilic triblock copolymers poly(butyl methacrylate)-*b*-poly(methacrylic acid)-*b*-poly-(butyl methacrylate) PBMA-*b*-PMAA-*b*-PBMA, consisting of hydrophobic end-blocks PBMA and hydrophilic mid-block PMAA, which form a hyperconnective physical network (B gel) by strong hydrophobic association of end-blocks PBMA (micelles). The glue-B gel is prepared by polymerizing the linear polyacrylamide (PAAm) (polymerization degree: $> 10^4$) with approximately 1:1 monomeric unit ratio to the mid-block PMAA in the B gel.(23) The linear PAAm chains associate with the mid-block chains through hydrogen bonding of their amino groups with the carboxyl groups of the PMAA, acting as efficient molecular glues of the network (Fig. 1a). The

detailed synthesis procedure of B gel and glue-B gel is shown in literature.(22, 24, 25)

Unless specifically mentioned, B gel made from PBMA-*b*-PMAA-*b*-PBMA with polymerization degree 93-302-93 for the three blocks will be discussed as a typical example. Each micelle in the B gel consists of 114 end-blocks and has a radius of 8.3 nm in average. About 60% of the end-blocks are connected to the neighboring micelles to constitute a network of hyperconnectivity with $f \cong 70$ strands of each micelle (see SI for details). The average distance between neighboring micelles (d_0) is 34.6 in B gel and it decreases to 22.7 nm in glue-B gel by introducing the PAAm linear chains (Fig. S1). The decrease in *d*-spacing of the glue-B gel is due to the shrinkage of the gel by hydrogen bond formation. At room temperature, the micelles were in glassy transition state.

The glue-B gel shows a quasi-linear stress-strain curve without prominent strain softening when being loaded uniaxially, with a strength significantly larger than that of the corresponding B gel (Fig. 1b). Specifically, at an initial strain rate of 0.01 s^{-1}, the B gel has a modulus of 0.04 MPa, fractures at a stress of 0.01 MPa and a stretching ratio λ of 1.30, while the glue-B gel has a modulus of 1.7 MPa, and sustains a stress up to 4.17 MPa and a stretching

ratio λ of 4.13. The prominent increase in modulus, fracture stress, and fracture strain of the glue-B gel is attributed to the formation of hydrogen bonding between the hyperconnective network and PAAm chains, which serves as dynamic crosslinks to dissipate energy.(22, 25)

The quasi-linear behavior is not limited to a specific loading rate but has been observed in a wide strain rate range. The stress level and fracture stress increase with the strain rate while the fracture stretching ratio hardly changes (Fig. S2a). Furthermore, the glue-B gels made from the triblock copolymers of different chain lengths (Tab. S1 and Fig. S2b) or of different preparation formulations (Fig. S2c) also show the similar non-softening, quasi-linear stress-strain behaviors. These results indicate that the observed behavior is a characteristic feature of glue-B gels. The non-softening, quasi-linear stress-strain relation in the whole deformation range makes the glue-B gels drastically different from conventional tough materials, which usually exhibit a prominent strain softening or even a necking phenomenon.(17, 26, 27)

To study the underlying molecular deformation mechanisms behind the unique mechanical behavior, we perform *in-situ* small-angle x-ray scattering (SAXS) during stretching of the B and glue-B gels. In these gels, the micelles not only act as multifunctional crosslinkers of the hyperconnective network

but also as nano-tracking beads for *in-situ* tracing of the network deformation when loaded, making them a perfect system for SAXS study. The B gel without deformation ($\lambda = 1.0$) shows isotropic scattering rings in SAXS pattern, demonstrating a random distribution of micelles (insets of Fig. 2a). Under stretching, the scattering ring from the correlation of micelles converts into an ellipse with its major axis perpendicular to the stretching direction, indicating that the *d*-spacing between adjacent micelles increases in the stretching direction and decreases in the perpendicular direction. Meanwhile, the scattering intensity concentrates in the stretching direction, suggesting that the periodicity of micelles improves in the stretching direction and deteriorates in the perpendicular direction with increasing deformation.(28) The scattering rings from the shape and size of micelles retain during deformation, indicating a negligible change in the structure of individual micelles. The evolution of SAXS patterns of glue-B gel is similar to that of B gel at small λ (insets of Fig. 2b), while four scattering spots appear at $\lambda > 1.75$, indicating the periodicity formed by micelles in specific directions.(29, 30)

The time-resolved SAXS patterns are quantified by extracting the *d*-spacing change along the directions parallel ($d_{//}$) and perpendicular ($d_{\perp}$) to the

stretching based on the anisotropic nature of the SAXS patterns (Figs. S3 and S4). From *d*-spacing change at each deformation, we calculate the microscopic deformation ratio of micellar network, d/d_0, and correlate it with the macroscopic deformation ratio λ. Here d and d_0 are the *d*-spacing at stretched and unstretched states, respectively. As the gels can be considered as incompressive materials in the observation timescale, when the network deformation equals the bulk deformation, $d_{//}/d_0 = \lambda$ and $d_{\perp}/d_0 = \lambda^{-0.5}$, where $d_{//}/d_0$ and $d_{\perp}/d_0$ are the network deformation ratios in the directions parallel and perpendicular to the stretching, respectively. Such deformation is known as affine deformation.

As shown in Fig. 2(a), for the B gel, even at a small stretch, e.g. $\lambda = 1.05$, $d_{//}/d_0 < \lambda$ and $d_{\perp}/d_0 > \lambda^{-0.5}$, which is named as sub-affine here. This sub-affine behavior indicates that the average deformation at the network scale in B gel is smaller than the bulk deformation. This result suggests that even at such small λ, strain amplification at some local places starts to appear, as a result of local structure damage. In contrast to the B gel, the glue-B gel maintains exactly the relation $d_{//}/d_0 = \lambda$ and $d_{\perp}/d_0 = \lambda^{-0.5}$ over the whole deformation range, indicating a perfect affine deformation of the nano-scale network up to the sample fracture (Fig. 2b). This surprising result indicates

that there is no local strain amplification at the polymer network length scale for the glue-B gel until sample failure. We should mention that $d_{\perp}$ for stretching ratio beyond 1.74 cannot be measured due to the poor periodicity of micelles in the perpendicular direction. The large affine deformation of the glue-B gel up to fracture is observed in all studied initial strain rates from 0.001 to 0.1 s^{-1} (Fig. S5), in consistent with their linear-like mechanical behaviors (Fig.S2a). This result further confirms that the unique non-softening behavior of glue-B gels is a characteristic feature originated from their unique polymer network structure.

Knowing that the B gel is quite brittle and fractures at small stretching, the skeleton network of glue-B gel should have structure damage during deformation despite the large affine deformation at polymer network scale. To confirm this, we performed cyclic test on the glue-B gel. The gel was loaded to a prescribed deformation, λ_{max}, followed by unloading at the same speed. The loading-unloading cycle was repeated several times after relaxation of different durations ranging from 3 s to 10^5 s. As shown in Fig. 3a, the loading-unloading curve of the original gel at $\lambda_{\max} = 1.70$ exhibited a large hysteresis. The partial recovery in stress while almost full recovery in sample length were observed after an enough waiting time of 10^5 s (Fig. 3b).

The partial stress recovery suggests that the large hysteresis stems from two contributions: reversible and irreversible structure damage. The former should be associated to the breaking and reforming of hydrogen bonds between the skeleton network and molecular-glue chains, while the latter is due to the irreversible damage of the network in the observation time window. The irreversible area increases with λ, suggesting that the irreversible damage increases with deformation (Figs. 3c and S6). We notice that the fraction of irreversible dissipation relative to the total work of stretch is almost constant (~0.3) even at relatively small λ (Fig. 3d). This behavior is quite different from DN gels in which the fraction of irreversible dissipation increases with the deformation before yielding.(31) As the glue polymers are not chemically crosslinked, the full recovery in sample length suggests that the skeleton network of the glue B gel maintains the percolated structure even after a large amount of irreversible damage, which is consistent with the large affine deformation of the glue-B gel.

The above result suggests a very different internal fracture process of glue-B gel from B gel and the conventional tough DN gels. That is, the internal rupture occurs dispersedly without causing stress concentration at the level of the micelle network, until the sample failure, while the B gel and the

conventional DN gels start to show sub-affine deformation even before yielding, indicating that internal fracture causes stress concentration at network level and most of the network carries less load even before yielding. (17, 18, 32) The ability to retain the affine deformation without stress concentration at the network scale of glue-B gels should be attributed to the interplay of hyperconnectivity of the skeleton network and the hydrogen bonding formed by glue polymers. To confirm this assumption, we further studied the behavior of a chemical gel (glue-C gel) made from the midblock polymer PMAA as the skeleton network, where each chemical crosslinking point connects four network strands, and the linear PAAm chains as molecular glues, which also forms hydrogen bonding with the PMAA strands (see SI for details). The glue-C gel with the same polymer density and modulus as that of the glue-B gel also shows improved fracture strength and fracture strain relative to its corresponding counterpart C gel (Fig. S7). While different from glue-B gel, the glue-C gel shows obvious strain softening behavior, suggesting that local strain amplification occurs in the glue-C gel without hyperconnectivity.

No measurable chain scission occurs in the glue-B gel before fracture, as demonstrated by mechanochemical color-changing test (see SI for details).

We consider that the irreversible structure damage is due to the pullout of the end-block chain from micelles. Indeed, we observe a rate-dependent mechanical behavior of the B gel (Fig. S8). The stress of B gel for λ smaller than 1.05 demonstrates no rate dependence, while the stress at λ larger than 1.05 increases with loading rate. This critical λ is the same as the λ that the B gel starts to show non-affine deformation. This indicates that the pullout of the end-block chains starts to occur at this critical λ due to dispersity and statistic distribution of the chains. Here, we estimate the axial force required to pullout an end-block chain from its micelle using the equation, $F_{pullout} = \zeta_0 \dot{\gamma} L$, where ζ_0 is the friction coefficient per unit length, $\dot{\gamma}$ is the deformation rate, L is the contour length of the end-block chain.(33) ζ_0 is 0.468 $N \cdot s \cdot m^{-1}$ around experimental temperature(34) and L is 14.3 nm from the molecular structure, thus the estimated maximum $F_{pullout}$ is only around 0.67 nN even for the highest $\dot{\gamma} = 0.1\ s^{-1}$ in this experiment, which is much smaller than the force to rupture the chemical bond of the chain (~4 nN).(35) This explains why the chain pullout occurs rather than the chain scission.

Next, we discuss what determines the failure stretch ratio λ_f of the glue B gel and why λ_f hardly depends on the strain rate while the fracture stress does in a wide strain rate range (0.001~0.1 s^{-1}) (Fig. S2a). Given the chain pullout

mechanism, λ_f is expected to increase with the strain rate since the pullout force is proportional to the loading rate, and the skeleton network should be stretched more at a larger force. To explain the behavior of λ_f, we estimated the chain conformation at sample fracture. By the affine deformation, the average inter-micelle distance at sample fracture $d = \lambda_f * d_0$, where d_0 is the inter-micelle distance without stretch. We estimated the normalized stretch length at fracture in relative to the total contour length L of the pulling out chain, $d/L = \lambda_f * d_0/L$. If we assume that when one end is pulling out from micelle, the other end of the chain is intact, then the total contour length L = 114 nm is the sum of one end-block chain (L = 14.3 nm) and one middle-block chain (L= 99.7 nm) (see SI). Using d_0 = 22.7 nm and the fracture stretch ratio λ_f = 3.6~4.5 at various strain rates (Figure S2a), d/L = 0.7~0.9. As the relatively short chains are pulled out first, the actual d/L value of the pullout chains might be even higher than the estimated value. This result indicates that the chains are highly stretched during the pulling out process. At this high stretch ratio, the force-extension relation of a chain is quite non-linear, and the force abruptly increases with the stretching.(36) This may explain why the fracture stress of the glue B gel depends on the strain rate while λ_f hardly does.

Combining the above results and discussion, we draw a cartoon to show deformation and internal damage mechanisms for the B and glue-B gels (Fig. 4). Like most of the network materials, the network of B and glue-B gels are not homogeneous due to the polydispersity of triblock copolymer ($M_w/M_n =$ 1.31 for whole chain). When loaded, the end-block with the shortest PMAA mid-block is pulled out from the micelle first, and the stress carried by the pullout strand redistributes among the intact strands. In the case of B gel (Fig. 4a), the stress redistributes to neighboring strands. This results in an increase of the force of the neighboring strands, which further causes pullout of the neighboring strands. As the strain is amplified locally in the damaged region, the rest of the network is less deformed to show the sub-affine deformation. With further increase of deformation, the damaged region grows, and when such local defect is increased to a critical value, it initiates an avalanche rupture process, resulting in catastrophic failure of the sample.

In the case of the glue-B gel, the glue polymers with a much longer polymer chains form physical hydrogen-bonds with multiple midblock chains of the hyperconnective network. When the shortest end-block chain is pulled out, stress redistribution is far more diffusive over many strands and over much longer length through the physically bonded glue linear chains. As a result,

the stress concentration at the position of the pullout chain hardly occurs. Consequently, with increasing deformation, further rupture does not occur at the neighboring strand, but occurs at the remaining shortest strands that are located randomly in the skeleton network. Through such a randomly dispersed strand breaking mechanism, the defect or microcrack does not grow and the crack propagation of the skeleton network is substantially suppressed. In addition, since each micelle is hyperconnected to about 70 strands, the micelle still carries load even many of its strands are pulled out. Accordingly, no significant strain softening or necking occurs, and the gel maintains the quasi-linear stress-strain relation up to sample failure (Fig. 4b). During this process, the chain pullout and breaking of hydrogen bonding dissipate a lot of energy and endow the gel a high toughness. Thus, the unique behavior of glue-B gel is an interplay of the hyperconnectivity of skeleton network and the glue polymers. Due to relatively large frictional resistance, the chains are stretched close to their full length during pulling out process from the micelles, which results in a large macroscopic failure strain.

This work provides insight for developing strong and tough hydrogels without prominent strain softening. That is, suppressing the stress concentration around the broken chain or a defect is important. For example,

in the DN gel, although introduction of the second network suppresses the stress concentration to a certain extent, stress concentration still exists. At necking, where the first network breaks into discontinuous phase, only about 1% first network strands break for a typical DN gel(21) and the yield stress is only several percent of the ideal fracture stress of the first network even for a DN gel with a quite homogenous first network.(17) These results indicate that stress concentration still severely exists around the broken strands in the DN gels. If the stress concentration can be completely suppressed, and the strands in the first network break in an order fully following the strand length statistics, the yielding stress and strain will significantly increase in the DN gels.

Conclusion

We have revealed that the tough glue-B gel maintains non-softening, quasi-linear deformation throughout the loading process, up to the failure of sample. This surprising phenomenon is attributed to the synergy of hyperconnectivity of the skeleton network and the efficient load transfer between the skeleton network and glue polymers. Consequently, the skeleton network maintains the integrality even after severe rupture of the network strands by chain pullout mechanism. As there is no obvious local stress concentration and strain

amplification during deformation, the gel does not show prominent strain softening or necking, but it shows a unique quasi-linear stress-strain relation with mechanical hysteresis in a wide observation window. This work provides a new strategy to design tough soft materials by combining hyperconnectivity network and molecular glues. Besides, this work provides deep insight for designing strong and tough hydrogels showing inelastic but large linear deformation. We believe the unique molecular mechanism proposed here changes our view on how soft materials deform in large strain and paves the way for future design of large linear deformation materials.

Materials and Methods

Materials: The amphiphilic triblock copolymer, poly(butyl methacrylate)-*b*-poly(methacrylic acid)-*b*-poly(butyl methacrylate) (PBMA-*b*-PMAA-*b*-PBMA) with polymerization degrees of 93-302-93, was synthesized by the Otsuka Chemical Co., Ltd., Japan. The monomers acrylamide (AAm) and methacrylic acid (MAA), the initiator 2-oxoglutaric acid (α-keto), and the solvent dimethylformamide (DMF) were purchased from Wako Pure Chemical Industries, Ltd., Japan.

Hydrogel preparation: The triblock copolymers were dissolved in dimethylformamide homogeneously at a concentration of 0.19 (wt/wt). Then

the solution was poured in a sample cell with a size of 80 (length) × 80 (width) × 2 mm (thickness). Gelation via hydrophobic association of the PBMA blocks was induced by spraying water vapor on the surface of solution for several minutes. The as-prepared gel was immersed in water for 3 days to reach equilibrium (denoted as B gel). The B gel was further immersed in an aqueous solution containing second monomer AAm (2 mol/L) and 2-oxoglutaric acid (0.05 mol% relative to the concentration of second monomer) as UV-initiator for 3 days, followed by the irradiation with 365 nm UV light for 8 h. After polymerization, the gel was immersed in pure water for 3 days to reach equilibrium (denoted as glue-B gel). The sample thickness of B gel and glue-B gel were 1.5 mm and 1.1 mm, respectively. The deswelling of glue-B gel in relative to B gel is due to the hydrogen bond formation.

For better comparison, the chemically crosslinked PMAA gel containing linear PAAm (glue-C gel) with the same polymer density and crosslinking density as glue-B gel was prepared as follows. The chemical skeleton network gel (C gel) was prepared from an aqueous solution containing 1.715 mol/L MAA monomer, 0.05 mol% 2-oxoglutaric acid and 5 mol% MBAA and polymerized under UV for 8 h. Then, the C gel was immersed in AAm solution (AAm 1.715 M, 2-oxoglutaric acid 0.05 mol %) for 3 days and

polymerized under UV for 8 h. The obtained gel was equilibrated in water for 3 days (glue-C gel). After that, the polymer density of glue-C gel was controlled as the same as that of glue-B gel with osmotic stress method.(37) The glue-C gel prepared at this condition has the same Young's modulus as glue-B gel.

Small-angle x-ray scattering (SAXS): The *in-situ* SAXS measurements were performed at BL19U2 beamline at the National Center for Protein Sciences Shanghai, China. The wavelength of x-ray was 1.033 Å and the sample-to-detector distance was set to be 6225.6 mm. A Pilatus 1M detector with a resolution of 981 × 1043 pixels (pixel size is 172 μm) was used to collect two-dimensional (2D) scattering patterns. A customized stretching device (provided by Puliang technology, Hefei, China) was used to stretch the sample, during which the stress and SAXS pattern were recorded. Constant stretching velocities from 0.02 mm/s to 2 mm/s were used to stretch the sample, which give initial strain rates from 0.001 to 0.1 s^{-1}. During measurement, the humidity (saturated water vapor) and temperature (25 ± 1 °C) around sample were well controlled. The samples with a rectangular shape with a gauge length of 20 mm, width of 7.5 mm and thickness from ~1.1 mm to ~1.5 mm were used. The data acquisition time was 20 s per frame for the

2D SAXS images. All scattering data were analyzed with Fit2D software from European Synchrotron Radiation Facility by taking off the detector spatial distortion, x-ray beam fluctuation and background scattering.

Cyclic test. The cyclic measurements with different waiting time were performed using a tensile-compressive tester (Tensilon RTC-1310A, Orientec Co.). The sample was stretched to a prescribed deformation, followed by the unloading at the same velocity. The stretching velocity is 0.2 mm/s, giving an initial strain rate of 0.01 s^{-1}. Other experimental conditions and the sample size were the same as that in SAXS experiment.

Acknowledgments

The authors thank Mr. Osamu Ito and Mr. Hiroyuki Ishitobi (Otsuka Chemical Co., Ltd.) for providing triblock copolymers and Prof. Liangbin Li for providing tensile device. The SAXS experiments were performed at NCPSS BL19U2 beamline at National Center for Protein Sciences Shanghai. This research was supported by JSPS KAKENHI Grant Numbers JP17H06144, JP17H06376 and JP19K23617. K. C and J. P. G. acknowledge Institute for Chemical Reaction Design and Discovery (ICReDD) established by World Premier International Research Initiative (WPI), MEXT, Japan.

References

1. F. P. Beer, E. R. Johnston Jr, J. DeWolf, D. F. Mazurek, Stress and strain–Axial loading. *Plant J, ed. Mech. Mater. 3rd ed. New York McGraw-Hill*, 48–57 (2001).

2. T. H. Courtney, *Mechanical behavior of materials* (Waveland Press, 2005).

3. M. D. Demetriou, *et al.*, A damage-tolerant glass. *Nat. Mater.* **10**, 123–128 (2011).

4. X. Liao, *et al.*, High strength in combination with high toughness in robust and sustainable polymeric materials. *Science (80-.).* **366**, 1376–1379 (2019).

5. Y. Zhang, *et al.*, Bioinspired, graphene-enabled Ni composites with high strength and toughness. *Sci. Adv.* **5**, 5577 (2019).

6. C. C. Hays, C. P. Kim, W. L. Johnson, Microstructure controlled shear band pattern formation and enhanced plasticity of bulk metallic glasses containing in situ formed ductile phase dendrite dispersions. *Phys. Rev. Lett.* **84**, 2901 (2000).

7. J.-Y. Sun, *et al.*, Highly stretchable and tough hydrogels. *Nature* **489**, 133–136 (2012).

8. J. P. Gong, Y. Katsuyama, T. Kurokawa, Y. Osada, Double-network hydrogels with extremely high mechanical strength. *Adv. Mater.* **15**, 1155–1158 (2003).

9. R. O. Ritchie, The conflicts between strength and toughness. *Nat. Mater.* **10**, 817–822 (2011).

10. Y. Tanaka, A local damage model for anomalous high toughness of double-network gels. *Epl* **78** (2007).

11. H. R. Brown, A model of the fracture of double network gels. *Macromolecules* **40**, 3815–3818 (2007).

12. J. P. Gong, Why are double network hydrogels so tough? *Soft Matter* **6**, 2583–2590 (2010).

13. C. Creton, 50th Anniversary Perspective: Networks and Gels: Soft but Dynamic and Tough. *Macromolecules* **50**, 8297–8316 (2017).

14. X. Zhao, Multi-scale multi-mechanism design of tough hydrogels: building dissipation into stretchy networks. *Soft Matter* **10**, 672–687 (2014).

15. X. Hu, M. Vatankhah-Varnoosfaderani, J. Zhou, Q. Li, S. S. Sheiko, Weak hydrogen bonding enables hard, strong, tough, and elastic hydrogels. *Adv. Mater.* **27**, 6899–6905 (2015).

16. T. L. Sun, *et al.*, Physical hydrogels composed of polyampholytes demonstrate high toughness and viscoelasticity. *Nat. Mater.* **12**, 932–937 (2013).

17. T. Matsuda, *et al.*, Yielding criteria of double network hydrogels. *Macromolecules* **49**, 1865–1872 (2016).

18. K. Fukao, *et al.*, Effect of Relative Strength of Two Networks on the Internal Fracture Process of Double Network Hydrogels As Revealed by in Situ Small-Angle X-ray Scattering. *Macromolecules* **53**, 1154–1163 (2020).

19. R. Long, C.-Y. Hui, Fracture toughness of hydrogels: measurement and interpretation. *Soft Matter* **12**, 8069–8086 (2016).

20. E. Ducrot, H. Montes, C. Creton, Structure of tough multiple network elastomers by small angle neutron scattering. *Macromolecules* **48**, 7945–7952 (2015).

21. T. Nakajima, T. Kurokawa, S. Ahmed, W. Wu, J. P. Gong, Characterization of internal fracture process of double network hydrogels under uniaxial elongation. *Soft Matter* **9**, 1955–1966 (2013).

22. H. J. Zhang, *et al.*, Tough Physical Double-Network Hydrogels Based on Amphiphilic Triblock Copolymers. *Adv. Mater.* **28**, 4884–4890 (2016).

23. R. V Ivanov, V. I. Lozinsky, S. K. Noh, S. S. Han, W. S. Lyoo, Preparation and characterization of polyacrylamide cryogels produced from a high-molecular-weight precursor. I. Influence of the reaction temperature and concentration of the crosslinking agent. *J. Appl. Polym. Sci.* **106**, 1470–1475 (2007).

24. Y. N. Ye, *et al.*, Relaxation Dynamics and Underlying Mechanism of a Thermally Reversible Gel from Symmetric Triblock Copolymer. *Macromolecules* **52**, 8651–8661 (2019).

25. Y. N. Ye, *et al.*, Tough and Self-Recoverable Thin Hydrogel Membranes for Biological Applications. *Adv. Funct. Mater.*, 1801489 (2018).

26. Z. Jiang, B. Diggle, I. C. G. Shackleford, L. A. Connal, Tough, Self-Healing Hydrogels Capable of Ultrafast Shape Changing. *Adv. Mater.* **31**, 1904956 (2019).

27. L. Tang, *et al.*, Double-Network Physical Cross-Linking Strategy To Promote Bulk Mechanical and Surface Adhesive Properties of Hydrogels. *Macromolecules* **52**, 9512–9525 (2019).

28. K. Cui, *et al.*, Multiscale energy dissipation mechanism in tough and self-healing hydrogels. *Phys. Rev. Lett.* **121**, 185501 (2018).

29. P. K. Challa, *et al.*, Viscoelastic properties of a branched liquid crystal in the nematic phase. *Liq. Cryst.* **41**, 747–754 (2014).

30. Z. Bartczak, A. Vozniak, WAXS/SAXS study of plastic deformation instabilities and lamellae fragmentation in polyethylene. *Polymer (Guildf).* **177**, 160–177 (2019).

31. R. E. Webber, C. Creton, H. R. Brown, J. P. Gong, Large strain hysteresis and mullins effect of tough double-network hydrogels. *Macromolecules* **40**, 2919–2927 (2007).

32. I. Kolvin, J. M. Kolinski, J. P. Gong, J. Fineberg, How supertough gels break. *Phys. Rev. Lett.* **121**, 135501 (2018).

33. B. R. Munson, T. H. Okiishi, W. W. Huebsch, A. P. Rothmayer, *Fluid mechanics* (Wiley Singapore, 2013).

34. J. D. Ferry, R. F. Landel, Molecular friction coefficients in polymers and their temperature dependence. *Kolloid-Zeitschrift* **148**, 1–6 (1956).

35. G. H. Michler, F. J. Balta-Calleja, *Mechanical properties of polymers based on nanostructure and morphology* (CRC Press, 2016).

36. M. D. Wang, H. Yin, R. Landick, J. Gelles, S. M. Block, Stretching DNA with optical tweezers. *Biophys. J.* **72**, 1335 (1997).

37. K. Cui, *et al.*, Effect of Structure Heterogeneity on Mechanical Performance of Physical Polyampholytes Hydrogels. *Macromolecules* **52**, 7369–7378 (2019).

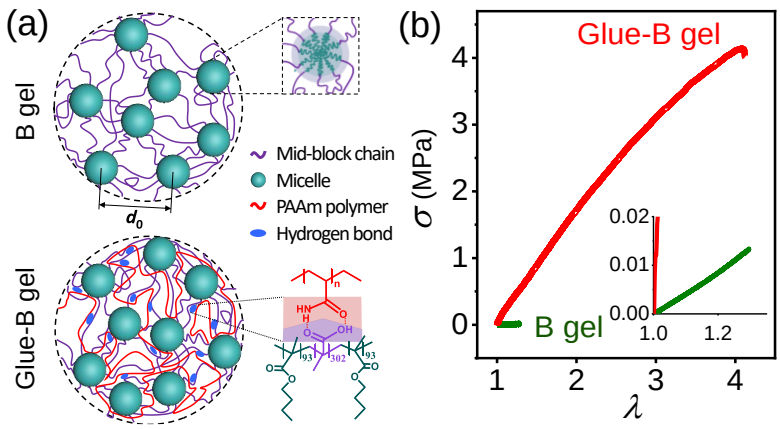

FIG. 1. Molecular structure and mechanical performance of B and glue-B gels. (a) Schematic diagram depicting the molecular structures of B and glue-B gels. B gel is formed from PBMA-*b*-PMAA-*b*-PBMA triblock copolymers. The PBMA end-blocks form micelles in water and serve as physical crosslinkers. The d_0 represents the average neighboring inter-micelle distance. The glue-B gel is formed by polymerizing PAAm inside the B gel, and the linear PAAm forms hydrogen bonding with the PMAA mid-block of the B gel. (b) Nominal stress-stretch curves for the B and glue-B gels in uniaxial tension. Samples have a rectangular shape with a gauge length of 20 mm and a width of 7.5 mm, and the initial strain rate was 0.01 s^{-1}. Inset in (b) shows the enlarged view of small stretch ratio.

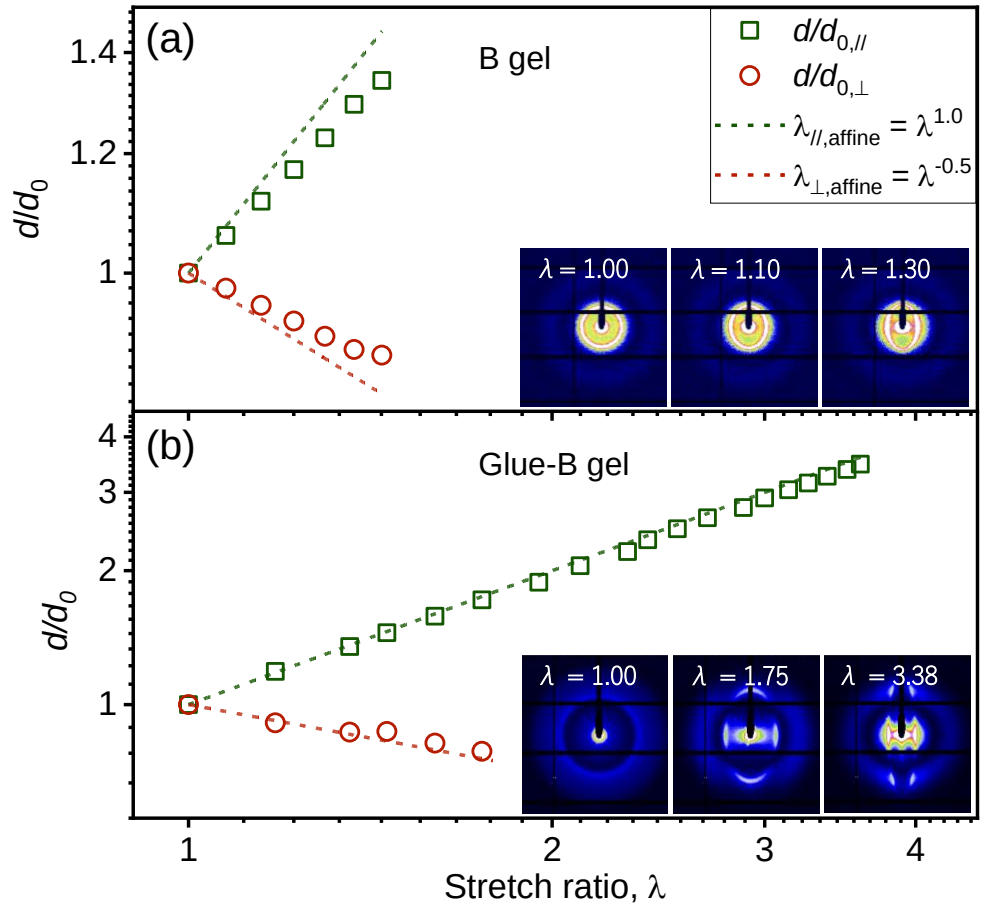

FIG. 2. Structure evolution of B and glue-B gels subjected to uniaxial tension as observed by *in-situ* SAXS measurement. The microscopic deformation ratio (d/d_0) in the parallel (//) and perpendicular ($\perp$) directions of stretching versus λ for (a) B gel and (b) glue-B gel. The insets are the 2D SAXS patterns at representative λ for B and glue-B gels. Initial strain rate: 0.01 s^{-1}. Stretching direction is horizontal.

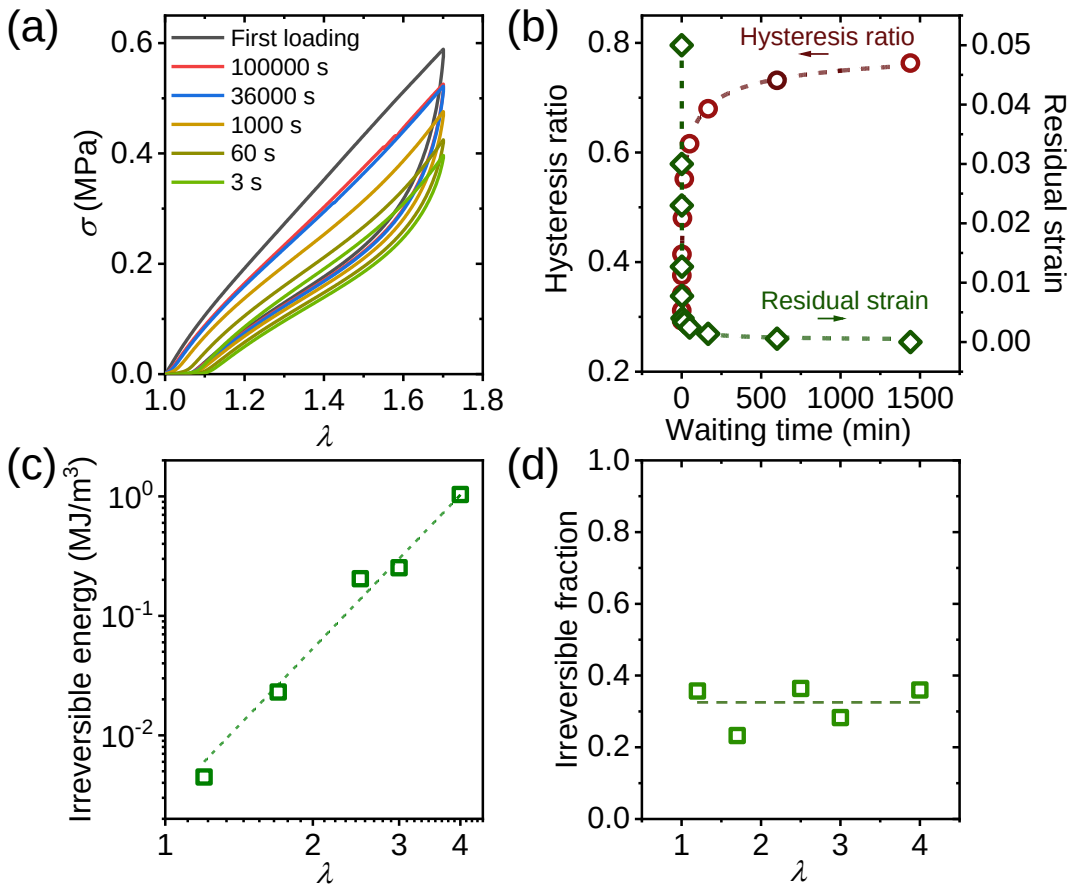

FIG. 3. Experiments depicting the irreversible internal breakage occurred by stretching in glue-B gel. The irreversible internal breakage means the damaged structure that cannot recover after a waiting time of 10^5 s. (a) Cyclic tensile test at different waiting times between the first and the subsequent cycles at a stretching ratio $\lambda = 1.7$. The initial strain rate was 0.01 s^{-1}. (b) Waiting time-dependencies of residual strain and recovery ratio defined as the area ratio of second hysteresis loop to the first one. (c) λ-dependence of the irreversible energy determined from the difference between the first hysteresis loop and the one that obtained after a waiting time of 10^5 s. (d) The fraction of the irreversible energy relative to the total work of stretch determined from the stress-strain curve.

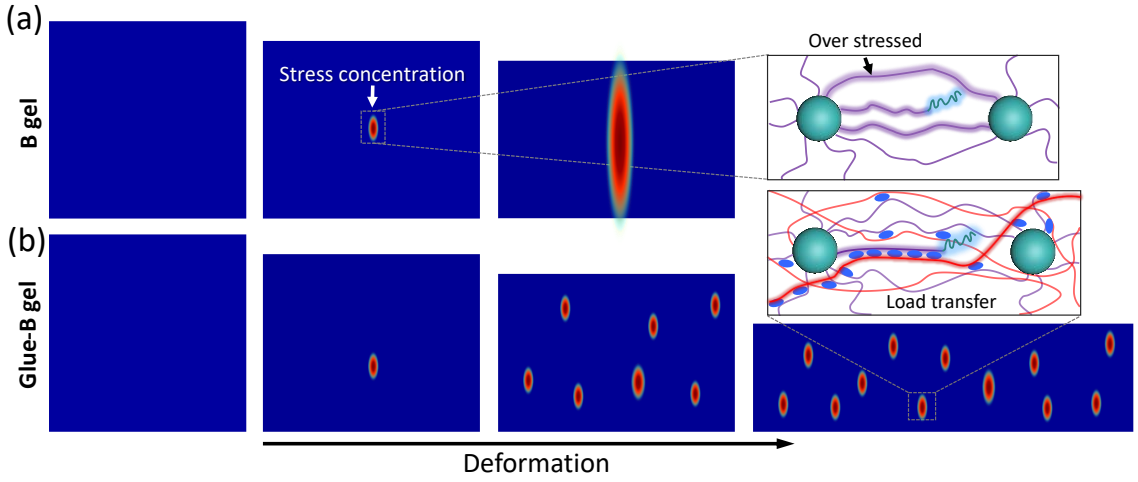

FIG. 4. Schematic to show the molecular mechanism of deformation and fracture of B and glue-B gels. For B gel, once the shortest strand is pulled out from micelle, the neighboring strands will be overloaded. The stress concentration amplifies the local strain and induces the catastrophic failure of the sample. Thus, the gel shows nonaffine deformation in its network and failures at small stretching. The bolded chains highlight the pullout chain and the overstressed neighboring chains. For the glue-B gel, when the shortest strand of network is pulled out, the load will be transferred to the glue polymers, which effectively suppress local stress concentration. With increasing deformation, further rupture does not occur at the neighboring strands but occur randomly in the skeleton network. At the same time, the hyperconnectivity retains the integrity of the skeleton network. Consequently, the gel always shows affine deformation in its network and quasi-linear stress-strain response. The bolded chains highlight the pullout chain and the load transfer from the pullout chain to glue polymer.